IRIS AperTO

UNIVERSITÀ DEGLI STUDI DI TORINO

AperTO - Archivio Istituzionale Open Access dell'Università di Torino

Stathmin expression modulates migratory properties of GN-11 neurons in vitro

This is the author's manuscript

Original Citation:

Availability:

This version is available http://hdl.handle.net/2318/1101 since

Published version:

DOI:10.1210/en.2004-0972

Terms of use:

Open Access

Anyone can freely access the full text of works made available as "Open Access". Works made available under a Creative Commons license can be used according to the terms and conditions of said license. Use of all other works requires consent of the right holder (author or publisher) if not exempted from copyright protection by the applicable law.

(Article begins on next page)

12 October 2024

0013-7227/05/$15.00/0
Printed in U.S.A.

Endocrinology 146(4):1825–1834
Copyright © 2005 by The Endocrine Society
doi: 10.1210/en.2004-0972

Stathmin Expression Modulates Migratory Properties of GN-11 Neurons *in Vitro*

Costanza Giampietro, Federico Luzzati, Giovanna Gambarotta, Paolo Giacobini, Enrica Boda, Aldo Fasolo, and Isabelle Perroteau

Department of Human and Animal Biology, University of Torino, 10123 Torino, Italy

Expression of stathmin, a microtubule-associated cytoplasmic protein, prominently localized in neuroproliferative zones and neuronal migration pathways in brain, was investigated in the GnRH neuroendocrine system *in vivo* and the function was analyzed using an *in vitro* approach. Here we present novel data demonstrating that GnRH migrating neurons in nasal regions and basal forebrain areas of mouse embryos express stathmin protein. In addition, this expression pattern is dependent on location, as GnRH neurons reaching the hypothalamus are stathmin negative. Immortalized GN-11 cells, which retain many characteristics of migrating GnRH neurons, strongly express stathmin mRNA and protein. The role of stathmin in GnRH migratory properties was evaluated using GN-11 cell line. We up-regulated [stathmin-transfected clones (STMN)+] and down-regulated (STMN−) the expression of stathmin in GN-11 cells, and we investigated changes in cell morphology and motility *in vitro*. Cells overexpressing stathmin assume a spindle-shaped morphology and their proliferation, as well as their motility, is higher with respect to parental cells. Furthermore, they do not aggregate and express low levels of cadherins compared with control cells. STMN− GN-11 cells are endowed with multipolar processes, and they show a decreased motility and express high levels of cadherin protein. Our findings suggest that stathmin plays a permissive role in GnRH cell motility, possibly via modulation of cadherins expression. (*Endocrinology* 146: 1825–1834, 2005)

GnRH NEURONS (also known as LH-releasing hormone, LHRH) control the release of anterior pituitary hormones, LH and FSH, in modulating the reproductive functions (1). In adult vertebrates, these neuroendocrine cells are scattered throughout the ventral forebrain and reside predominantly in the septal-preoptic and anterior hypothalamic areas (2). During embryonic development, GnRH cells originate in the nasal placode and migrate along olfactory/vomeronasal pathway to their final locations into the brain (3). Although the migration of these cells, from nose to brain, has been well documented in a variety of species (4–10), many questions remain concerning the molecules and cues directing GnRH cell migration.

Cell migration is a complex cellular behavior that results from the coordinated changes in the cytoskeleton and the controlled formation and dispersal of adhesion sites. Whereas the actin cytoskeleton provides the driving force at the cell front, the microtubule (MT) network assumes a regulatory function in coordinating rear retraction (11). Cytoskeletal rearrangements are crucial for all these events. For example, leading edge extension depends on polymerization of actin microfilaments, and nuclear translocation and retraction of the trailing edge involve MT assembly and disassembly, respectively (12). Stathmin (13) is a member of a class of MT destabilizing proteins that regulate the dynamics of MT polymerization/depolymerization and plays a critical role in the regulation of the dynamic equilibrium of MTs during different phases of the cell cycle (14–19) in a phosphorylation-dependent manner (14, 16, 20). The MT-destabilizing activity of stathmin is turned off by cell surface receptor kinase cascades and cycle-dependent kinases (21–25).

In the adult nervous system of mammals, relevant neurogenesis occurs in restricted areas, such as the olfactory epithelium (OE), the subependymal layer, and the dentate gyrus of the hippocampus (26, 27). Previous studies have demonstrated a high level of stathmin expression in these regions, supporting the idea that this protein is involved in processes of migration and differentiation (28). Interestingly, stathmin expression has been documented in the developing main OE and vomeronasal organ during mouse embryonic development as well as in populations of migrating cells crossing the nasal mesenchyme at early stages of development and resembling, for morphology and location, GnRH neurons (29). Here we show that stathmin is expressed in migrating GnRH neurons *in vivo* and in immortalized highly migratory GnRH neurons (GN-11 cells). Furthermore, using stable transfected GN-11 cells in which stathmin was up- or down-regulated, we show that stathmin specifically modulates motility properties of GN-11 cells.

Materials and Methods

All reagents were purchased from Sigma-Aldrich (St. Louis, MO) unless otherwise specified.

Animals and tissue

The experiments were carried out on CD-1 mice (Charles River, Lecco, Italy).

First Published Online December 29, 2004

Abbreviations: CNS, Central nervous system; E0, embryonic d 0; FBS, fetal bovine serum; GAPDH, enzyme glyceraldehyde-3-phosphate dehydrogenase; HGF/SF, hepatocyte growth factor/scatter factor; -ir, immunoreactivity; MT, microtubule; OE, olfactory epithelium; P30, postnatal d 30; SFM, serum-free medium; STMN, stathmin-transfected clones.

***Endocrinology* is published monthly by The Endocrine Society (http://www.endo-society.org), the foremost professional society serving the endocrine community.**

All animal protocols were approved by the Animal Care and Use Committee of the University of Turin.

Embryos

Timed pregnant mice [plug day, embryonic d 0 (E0)] were deeply anesthetized and killed at specified embryonic days. Embryos were harvested and washed in ice-cold Dulbecco's PBS. The heads were fixed in fresh 0.1 M (pH 7.4) PBS and 4% paraformaldehyde overnight at 4 C and cryoprotected in sucrose solution the next day. Tissues were then embedded in Killik frozen section medium (Bio Optic, Milan, Italy) and frozen in liquid nitrogen-cooled isopentane. Sagittal sections were cut, mounted on 3-aminopropyl-trietoxysilane-treated slides (Fluka, Milan, Italy) and stored at −20 C until processing for immunohistochemistry.

Adult mice

Adult CD-1 mice postnatal d 30 (P30) were anesthetized with an ip injection of ketamine (200 mg/kg), and perfused with 4% paraformaldehyde. The brains were dissected and postfixed in the same fixative overnight at 4 C, cryoprotected in sucrose solutions and sectioned on a cryostat. Sagittal sections were cut, mounted on 3-aminopropyl-trietoxysilane-treated slides (Fluka) and stored at −20 C until processing for immunohistochemistry.

Eight-micrometer-thick sections were used for consecutive mirror reactions, and 14-μm-thick sections were used for simultaneous double-labeling reactions.

Cell cultures

GN-11 cells (30) were grown in monolayer at 37 C in a humidified atmosphere of 5% CO_2/air, in DMEM (4500 mg glucose) containing 1 mM sodium pyruvate, 2 mM glutamine, 100 μg/ml streptomycin, 100 U/ml penicillin, and supplemented with 10% fetal bovine serum (FBS, Invitrogen Life Technologies, Inc., Grand Island, NY). The medium was replaced at 2-d intervals. Subconfluent cells were routinely harvested by trypsinization and seeded in 57-cm^2 dishes (1×10^6 cells).

Plasmids construction

DNA manipulations were carried out using standard techniques (31). cDNA fragments containing the entire coding region of rat stathmin were amplified by RT-PCR. The primers used (produced by Sigma-Genosys) were designed according to the rat GenBank stathmin sequence (accession no. J04979): 5′-TGTCTTCTGTCCAACATGGC-3′ and 5′-AAAACATCTCACGGTCTGGA-3′ corresponding to nucleotides 154–766. The obtained fragments were purified from agarose gel using GenElute Gel Purification Kit and cloned into the pGEM-T Vector System (Promega Corp., Madison, WI) following the manufacturer's instructions; the target DNA amplification fragment was then sequenced. The DNA of single colonies was obtained using GenElute Plasmid Miniprep Kit and subcloned into the *Eco*RV gap of pIRESpuro2 Vector (CLONTECH Laboratories, Palo Alto, CA). Stathmin antisense and stathmin sense expression vectors were identified by *Xba*I restriction map and denoted respectively pSTATHMIN− and pSTATHMIN+.

Plasmid transfection and generation of stable cell lines

pSTATHMIN−, pSTATHMIN+ and pIRESpuro2 empty vector, as a control, were transfected in GN-11 cells. Transfections were performed using Lipofectamine Reagent transfection reagent (Invitrogen Life Technologies) and Optimem (Invitrogen Life Technologies) according to the manufacturer's instruction. Briefly, cells were seeded in 100-mm tissue culture plates 1 d before transfection. The cell cultures, 60–80% confluent, were transfected with 10 μg plasmid DNA per plate for 4 h. After 48 h incubation in the appropriate growth medium, the selection of clones was carried out for 2 wk in 10 μg/ml puromycin. About thirty different clones were collected and assayed for stathmin expression; clones expressing high or low stathmin levels were denoted, respectively, stathmin-transfected clones (STMN)+ or STMN− cells.

Immunohistochemistry

Consecutive E12 and P30 mouse sagittal sections (8 μm) were stained for GnRH and stathmin immunoreactivity. GnRH neurons were labeled using a rabbit polyclonal anti-GnRH antibody (LR5; a generous gift from Dr. Benoit, Montreal, Canada) at a 1:10,000 dilution, whereas stathmin immunoreactivity was detected using a rabbit polyclonal stathmin antiserum (a generous gift from Dr. Sobel, Paris, France) at a 1:1000 dilution. Sections were incubated overnight at 4 C with the mentioned antibodies diluted in 1% normal goat serum and 0.3% Triton X-100 in PBS. Sections were then washed in PBS and incubated with antirabbit biotinylated secondary antiserum and the Vector kit (ABC kit, Vector Laboratories, Burlingame, CA) and processed for avidin-biotin-horseradish peroxidase/3′-3-diaminobenzidine histochemistry. Sections were then washed in PBS, mounted, and coverslipped. Negative controls were run by omitting the primary antibody.

E12, E18, and P30 mouse sagittal sections (14 μm) were double-labeled for GnRH and stathmin immunoreactivity. Sections were incubated overnight at 4 C with the mentioned antibodies diluted in 1% normal goat serum and 0.3% Triton X-100 in PBS. The next day, sections were washed in PBS and incubated for 1 h with anti-Rb-Cy2-conjugated antibody (1:500, Jackson ImmunoResearch, West Grove, PA), washed in PBS, mounted and coverslipped. For double-labeling reactions, anti-GnRH/anti-stathmin, the AffiniPure Fab Fragment goat antirabbit IgG (H + L) (FabBlocker, Jackson ImmunoResearch) was used according to the manufacturer's protocol.

Labeled sections were mounted, air-dried, and coverslipped in polyvinyl alcohol with the anti-fading mounting medium diazabicyclooctane. Fluorescent signals were detected using a FV 200 Olympus Fluoview confocal laser scanning microscope (Olympus Corp., Hamburg, Germany). Only adjustment to brightness and contrast were used in the preparation of the figures.

For immunocytochemical analysis of STMN mutants, cells were grown on glass dishes in 10% FBS DMEM. After 24 h, cells were washed twice with PBS, and fixed for 6 min in 100% methanol at −20 C. MT networks were visualized using the α-tubulin antibody (mouse monoclonal 1:1000, Sigma-Aldrich) and the anti-Ms-Cy3-conjugated antibody (1:500, Jackson ImmunoResearch). Labeled cells were observed on an IX50 inverted microscope (Olympus Corp.) equipped with a charge-coupled device camera CoolSNAP-Pro (Media Cybernetics, Houston, TX) and images edited with Image Pro-Plus software (Media Cybernetics).

RT-PCR analysis

Total RNA was isolated by extraction with TRIzol (Invitrogen Life Technologies). Single-strand cDNA was synthesized by Moloney murine leukemia virus reverse transcriptase from 1 μg of total RNA primed with 50 pmol of random hexamers (Amersham Biosciences, Piscataway, NJ) in a 20-μl reaction. Each reaction consisted of Life Technologies' first-strand cDNA synthesis buffer [50 mM Tris-HCl (pH 8.3), 75 mM KCl, 3 mM $MgCl_2$], 4 mM deoxynucleotide triphosphates (Amersham Biosciences), 1.8 U/μl RNAsin (Amersham Biosciences) and 10 U/μl Moloney murine leukemia virus reverse transcriptase (Invitrogen Life Technologies). Samples were incubated at 37 C for 1 h. Negative controls: (RT−) were those in which reverse transcriptase was not added; (H_2O) were those in which sterile water instead of cDNA was added.

PCR was carried out using 5 μl of cDNA and the appropriate oligonucleotides (0.6–6 μM) in a 30-μl PCR using standard reaction buffer [10 mM Tris-HCl (pH 8.3), 50 mM KCl, 1.5 mM $MgCl_2$, 0.001% gelatin], 0.8 mM deoxynucleotide triphosphates (Amersham Biosciences) and 0.025 U/μl of REDTaq DNA polymerase.

The following primers were used: 5′-TGGCATTGTGGAAGGGCTCATGAC-3′ and 5′-ATGCCAGTGAGCTTCCCGTTCAGC-3′ for GAPDH amplification corresponding to nucleotides 544–732 (accession no. M32599); 5′-TGTCTTCTGTCCAACATGGC-3′ and 5′-AAAACATCTCACGGTCTGGA-3′ for stathmin amplification corresponding to nucleotides 154–766 (accession no. J04979); 5′-GGGACTGCAGCAGCAAAGC-3′ and 5′-GTCTGAGCATCTAGAGTTTCC-3′ for c-Met amplification corresponding to nucleotides 296–815 (32). The amplification of GAPDH served as a control with respect to the quality and quantity of RNA that had been retro-transcribed into cDNA. The number of cycles and the annealing temperature used for each primer pair were: 30 cycles at 57 C for stathmin, 25 cycles at 62 C for c-Met, and 25 cycles at 60 C

for GAPDH. Amplification products were separated by 1.5% agarose gel electrophoresis and DNA bands visualized by ethidium bromide staining.

Western blot analysis

For Western blotting analysis, GN-11 cells were solubilized in lysis buffer [Tris-HCl (pH 7.4), 100 mM NaCl, 5 mM $MgCl_2$, 0.5% NaDOC, 1% Nonidet P-40, 1 mM phenylmethylsulfonyl fluoride, 2 mM orthovanadate] on ice. Lysates were clarified by centrifugation at 14,000 × *g* for 15 min and protein content determined using a bicinchoninic acid kit for protein determination.

Equal amounts of proteins were boiled in Laemmli buffer [2% sodium dodecyl sulfate, 50 mM Tris-HCl (pH 7.4), 20% β-mercaptoethanol, 20% glycerol] and subjected to 8% (cadherins and c-Met) and 15% (stathmin) SDS-PAGE. Proteins were blotted onto Hybond-C Extra membrane (Amersham Biosciences).

After blocking with 5% dry milk in TBST buffer [20 mM Tris, 150 mM NaCl, 0.1% Tween 20 (pH 7.4)] filters were probed with 1:500 monoclonal ANTI-PAN cadherin antiserum, or 1:500 polyclonal c-Met antiserum (Santa Cruz Biotechnology, Inc., Santa Cruz, CA), or 1:10,000 polyclonal antistathmin antibody, or 1:1000 monoclonal β-actin antiserum (Sigma-Aldrich) and visualized with the appropriate peroxidase-coupled secondary antibodies using ECL detection system (Amersham Biosciences).

Proliferation assay

Cellular proliferation was quantified with the 96-well plates technique as previously described (33, 34). Briefly, cells were plated in 200 μl serum-free medium (SFM) at a density of 1000 cells/well in 96-well plates. The following day (t = 0), the medium was replaced by 100 μl/well SFM with or without 50 ng/ml of human recombinant hepatocyte growth factor/scatter factor (HGF/SF); for each treatment, eight wells were used. At t = 0, a 96-well plate was fixed and used as a cell growth start point. Cell growth was subsequently calculated at 1 d (t = 24 h), 2 d (t = 48 h), and 3 d (t = 96 h) after the initiation of treatments. The medium was removed and cells were fixed by addition of 100 μl 2% glutaraldehyde in PBS. After being shaken (200 cycles/min) for 20 min at room temperature, plates were washed five times by submersion in deionized water and air dried at least 24 h. Plates were then stained by addition of 100 μl/well of a solution containing 0.1% crystal violet dissolved in freshly prepared 200 mM boric acid at pH 9.0. After being shaken (200 cycles/min) for 20 min at room temperature, plates were washed five times by submersion in deionized water and air dried at least 24 h. Bound dye was solubilized by addition of 100 μl/well of 10% acetic acid and 5 min shaking at room temperature. The OD of dye extracts was measured directly in plates using a Microplate Reader (Bio-Rad, Hercules, CA), at the wavelength of 590 nm.

Morphological analysis of stable transfected clones

To classify and analyze different morphologies displayed by STMN+, pIRES and STMN− cells, Image Pro-Plus (Media Cybernetics) and Photoshop 7.0 software were used. Random cells were photographed using a 1 × 50 inverted microscope (Olympus Corp.) equipped with a charge-coupled device camera CoolSNAP-Pro (Media Cybernetics). For morphometric analysis cell body boundaries were manually traced with processes extending from cell bodies being not taken into account for measurements. Area, perimeter, maximum and minimum diameter of each cell were calculated using the software Image Pro-Plus (Media Cybernetics). Moreover, for each cell the ratio between maximum and minimum diameter of the cell body was evaluated. The measures were obtained considering only interphasic cells. All data were collected and statistically analyzed.

Motility assay

To measure two-dimensional movement, cells were plated at low density in culture dishes. The day after plating, cells (in DMEM-10% FBS) were photographed every 30 min for 3 h, and motility was analyzed as nuclear movement measurements. Photographs were aligned using Reconstruct Software version 1.0.2.0 (http://synapses.bu.edu/tools) and nuclear coordinates were measured using ImageJ Software National Institutes of Health (http://rsb.info.nih.gov/ij/). All the data were collected and statistically analyzed.

Aggregation assay

Cells aggregates were prepared by the hanging drop technique (35). Subconfluent cells were collected by trypsinization, resuspended in complete culture medium, and 20 (5) cells were seeded in 20-μl drops on the lid of a culture dish; the lid was then placed on a 35-mm dish filled with 2 ml of culture medium and incubated at 37 C for 48 h.

Collagen gel was obtained as previously described (36) and 200 μl were pipetted onto the bottom of a well of a 24-well culture dish, and left to set at room temperature. Cells aggregates were transferred over the cushion and then overlaid with additional 200 μl of collagen and covered with culture medium; aggregates were then photographed after 1 h.

Migration assay

The Transwell migration assay was used to measure three-dimensional movement. Cells (10^5) were seeded on the upper side of a Falcon cell culture insert (Becton Dickinson Labware, Franklin Lakes, NJ) on a porous polycarbonate membrane (8 μm pore size, 1 × 105 pores/cm^2) (37); the lower chamber of the cell plate was filled with serum-free DMEM or with serum-free DMEM containing 50 ng/ml of human recombinant HGF/SF. After 6 h of incubation, cells attached to the upper side of the filter were mechanically removed, whereas cells that migrated to the lower side of the filter were fixed in PBS 1% glutaraldehyde, stained with toluidine blue, photographed (4 mm^2/sample) and counted using Image Pro-Plus software (Media Cybernetics).

Statistical analysis

The experiments were performed in triplicates, and all counts obtained from assays were analyzed, averaged, and expressed as mean ± SE. SAS software (Cary, NC) was used for statistical analysis. Two-way ANOVA was performed. *Post hoc* tests were used to determine where statistically significant differences were located among the groups (Bonferroni, Tukey). The level of significance, unless otherwise indicated, was $P \leq 0.01$.

Results

Stathmin is expressed by migrating GnRH neurons in situ

Stathmin expression in the GnRH system was studied in mouse at embryonic stages E12 and E18 and in young adults (P30) by immunohistochemistry. The analysis was performed using either single-labeling immunohistochemistry on consecutive sections (8 μm apart) or double-labeling immunofluorescence on the same section, We showed that GnRH neurons migrating through the nasal mesenchyme during early stages of development express stathmin (Fig. 1).

At E12, stathmin-immunoreactivity (-ir) was detected in cells emerging from the presumptive vomeronasal organ and migrating in cords-like clusters toward the forebrain (Fig. 1A). To assess the relationship between GnRH and stathmin immunolabeling, the consecutive section was stained with anti-GnRH antiserum (Fig. 1B).

Stathmin staining pattern paralleled the GnRH neuronal distribution in the nose at this developmental stage. GnRH-ir overlapped partially with that for stathmin even though stathmin expression appeared not to be restricted to GnRH neurons. Confocal analysis of double labeling reaction on sagittal brain sections at the same embryonic stage confirmed the colocalization of GnRH and stathmin in the same cell body (Fig. 1, C–E). At E18, such colocalization was still detectable in GnRH neurons crossing the crybriform plate, entering the developing forebrain and moving through the

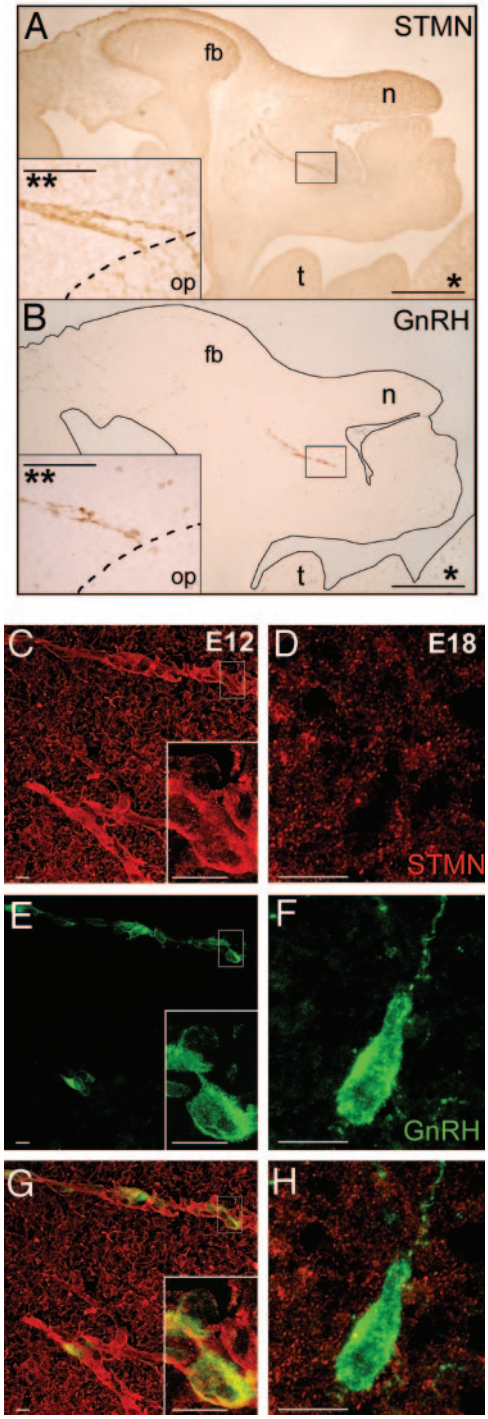

FIG. 1. Stathmin and GnRH *in vivo* immunohistochemistry. A and B, Immunohistochemistry for stathmin (A) and GnRH (B) performed on consecutive sagittal sections of a E12 mouse embryo. Immunoreactive cells emerged from the developing OE and migrate in chains through the olfactory mesenchyme toward the forebrain. Stathmin immunoreactivity resembles the staining pattern of GnRH. Note that the stathmin antibody likely labels the same groups of migrating elements stained with the GnRH antiserum. fb, Forebrain; n, nose; op, olfactory placode; t, tongue. *Scale bars*: *, 500 μm; **, 100 μm. C–E, Double simultaneous immunohistochemical staining for stathmin (C) and GnRH (D) at E12 in the nasal mesenchyme. A complete colocalization between stathmin and GnRH is shown in panel E (merge of C and D). *Scale bars:* 10 μm. F–H, Double simultaneous immunohistochemical staining for stathmin (F) and GnRH (G) at E18 in the hypothalamus. As shown in panel H (merge of F and G), no colocalization between stathmin and GnRH was observed in this region. *Scale bars*, 10 μm.

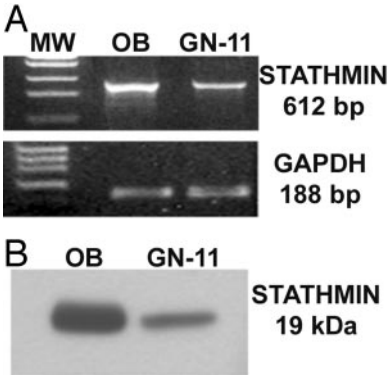

FIG. 2. Stathmin expression in GN-11 cell line extracts. A, Total GN-11 mRNA was assayed by RT-PCR for stathmin, GAPDH served as control. Predicted amplicons molecular weights were: 612 bp for stathmin and 188 bp for GAPDH. B, GN-11 cells protein extracts were analyzed for stathmin (19 kDa) expression. MW, Molecular weight; OB, olfactory bulb (positive control).

basal forebrain directed toward the hypothalamic regions (data not shown). At this stage, within these latter locations most GnRH neurons are stathmin negative (Fig. 1, F–H). Accordingly, at P30, when all the GnRH neurons are fully differentiated, no stathmin-ir can be detected in GnRH cells in any brain regions (data not shown). These results show that GnRH neurons express stathmin and that this expression is restricted to their migratory process being downregulated as the cells reach their final destinations. To further assess the relationship between stathmin expression and the migratory activity of GnRH neurons, we switched to an *in vitro* model using the GnRH immortalized cell line, GN-11.

GN-11 cells express stathmin

To use the GN-11 cell line for functional studies, we verified that this system retained expression of stathmin comparable to that observed *in vivo*.

RT-PCR (Fig. 2A), Western blot (Fig. 2B) and immunocytochemistry (not shown), demonstrated that stathmin is constitutively expressed by GN-11 cell line. RT-PCRs for stathmin transcripts yielded predicted 612-bp amplicons (Fig. 2A) and Western blotting analysis evidenced the expression of the 19-kDa stathmin protein (Fig. 2B) in GN-11 extracts. Olfactory bulb extracts were used as positive controls (28) and GAPDH amplification confirmed that equal amounts of RNA were included in each RT-PCR.

Stathmin transfections on GN-11 neurons modify the level of stathmin expression

The cDNA coding for stathmin (produced by RT-PCR) was cloned in pGEM-T vector and sequenced. The amplified cDNA differs from the published sequence (J04979) for nucleotides 210 and 526, but encodes for stathmin protein with 100% amino acidic sequence homology. The amplified cDNA was subcloned in sense or antisense direction in pIRESpuro2 expression vector and transfected in GN-11 cells. Twenty-

three sense (STMN+), seven antisense (STMN−), and 25 empty vector (pIRES) stable clones were selected by puromycin treatment and analyzed for stathmin expression at RNA (Fig. 3A) and protein level (Fig. 3B). Transfection of the vector containing sense stathmin cDNA allowed transcription of stathmin mRNA, leading to an increase in stathmin protein content (STMN+) compared with control (pIRES), whereas transfection of the vector containing antisense stathmin cDNA, leading to production of a mRNA complementary to the endogenous mRNA, knocked down significantly stathmin expression in these transfected cells (STMN−; Fig. 3B). To exclude unspecific effects of the stathmin expression vectors, STMN transfectants were analyzed the for transcript levels of stathmin-unrelated genes, such as the two tyrosine-receptors c-Met (38) and ErbB2 (39, 40) and the transcription factor activator protein-2α (41), which are expressed in the GN-11 parental cells. c-Met transcript levels (see Fig. 8) were unchanged in between STMN−, STMN+ and pIRES cells. Unaltered levels were also observed for ErbB2 and activator protein-2α (not shown).

Stathmin down-regulation modifies cell proliferation

The proliferation rate of stathmin transfectants was analyzed using crystal violet staining (see *Materials and Methods*). Clones in which stathmin was down-regulated (STMN−) exhibited a proliferation activity significantly reduced compared with control (pIRES; Fig. 4). Conversely, no significant difference in the growth rate of STMN+ clones was observed compared with control. The growth rate of control (pIRES) was similar to that of untransfected parental GN-11 cells (not shown).

Stathmin expression and cell morphology

Transfection of stathmin constructs induced significant morphological changes. STMN+ cells displayed a spindle-shaped body (bipolar) with the extension of two leading processes, whereas STMN− displayed a multipolar morphology (Fig. 5, A and E). pIRES cells, which express an intermediate level of stathmin compared with STMN+ and STMN− clones, exhibited both bipolar and multipolar morphologies (Fig. 5C). Quantitative morphological analysis was performed, taking into account diameter, area, and perimeter of random cells (n = 249 for STMN+ cells; n = 228 for pIRES cells; n = 323 for STMN− cells) for each clone (Fig. 6). The mean ratio between the maximum and minimum diameter (± SEM) was calculated. These values were 4.8 ± 0.14 μm for STMN+ clones, 3.2 ± 0.11 μm for pIRES and 2.6 ± 0.05 μm for STMN−, confirming that a significant difference in cell morphology existed between the three clones of transfected cells ($P < 0.01$).

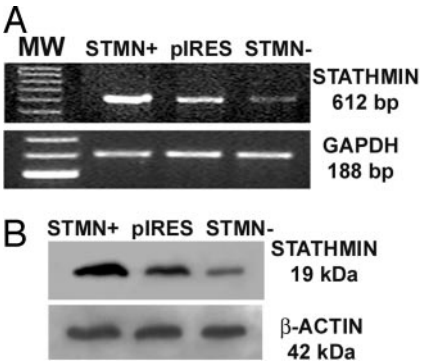

FIG. 3. Representative stathmin expression in STMN stable transfectants. A, Total mRNAs were assayed by RT-PCR for stathmin, GAPDH served as control. Predicted amplicons molecular weights were: 612 bp for stathmin and 188 bp for GAPDH. B, Total proteins from STMN+, pIRES and STMN− cells were assayed by Western blot analysis for stathmin. β-Actin served as control of the quantity of proteins.

FIG. 4. Effect of stathmin level modulation on cell proliferation in SFM culture condition. Lower levels of cells proliferation were found in conditions of lower level of stathmin (STMN− cells) (see *Materials and Methods*).

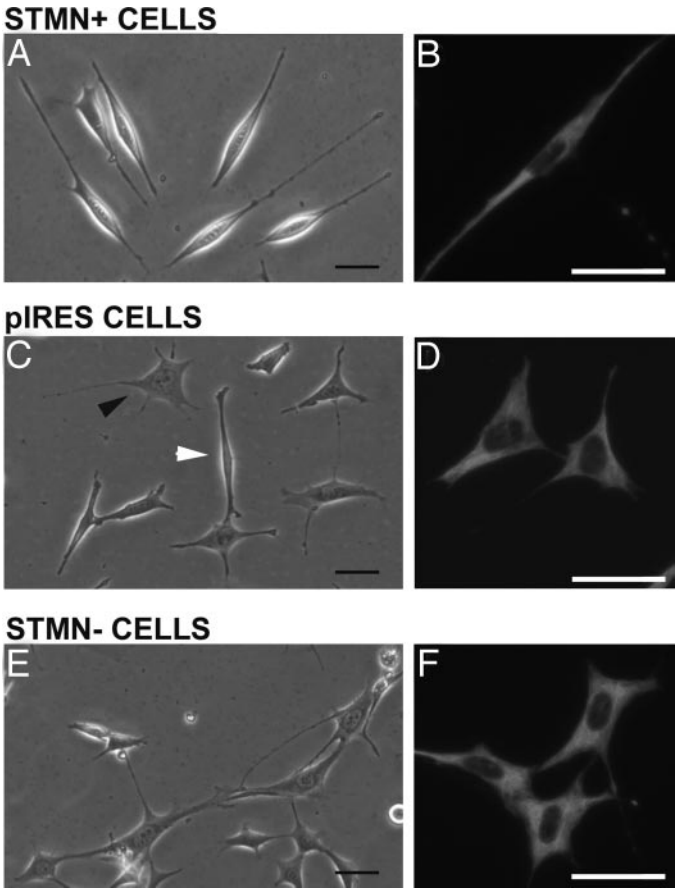

FIG. 5. Morphological characteristics of STMN stable transfectants. STMN+ cells displayed a spindle-shaped body with the extension of two leading processes (A), whereas STMN− were much more spread (E). pIRES cells (C), which express an intermediate level of stathmin compared with STMN+ and STMN− clones, exhibited both spindle (*white arrow*) and spread (*black arrow*) morphology. All the STMN transfectants (B, D, and F) exhibit intact MT networks, as shown by α-tubulin-ir. *Scale bars*, 20 μm.

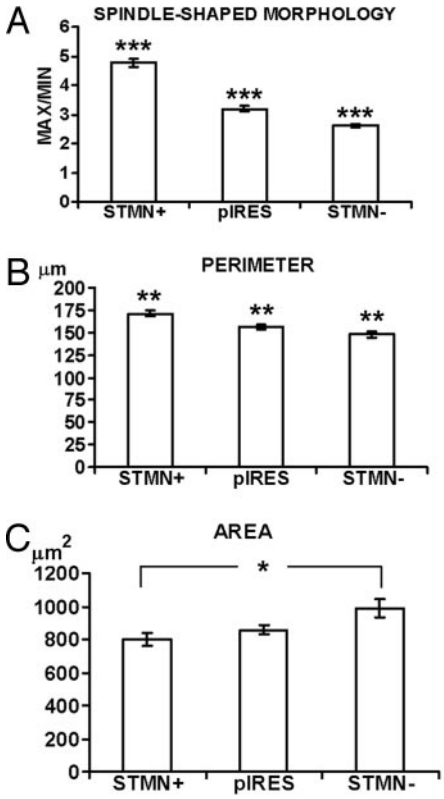

FIG. 6. Quantitative analyses of STMN stable transfectants morphological parameters. The morphometric data of every cell soma were measured semiautomatically: cell body boundaries were manually traced. For each cell body, spindle-shaped morphology (A) (evaluated as ratio between maximum and minimum diameter), perimeter (B), and area (C) were analyzed. Each value represents the mean ± SE; n = 249 STMN+ cells; n = 228 pIRES cells; n = 323 STMN− cells. Statistically significant differences of each group with one another were observed when comparing data concerning spindle-shaped morphology and perimeter (A and B). When comparing data concerning areas, statistically significant differences were observed only between STMN+ and STMN− cells (C).

Mean cell perimeters (±SEM) of clones STMN+, pIRES and STMN− were 171.3 ± 3.1 μm; 155.9 ± 2.4 μm; 147.8 ± 3.2 μm, respectively. Statistical analysis evidenced a significant difference ($P < 0.05$) of cell perimeters between STMN+ and pIRES, STMN− and pIRES, STMN+ and STMN− clones, respectively. Mean cell body areas (±SEM) of clones STMN+, pIRES, and STMN− were 798.8 ± 41.6 μm; 857.8 ± 25.4 μm; 987.2 ± 54.7 μm. Statistical analysis showed significant difference ($P < 0.05$) between STMN+ and STMN− clones.

To test whether the overexpression of stathmin is associated with abnormal MTs, STMN cells were immunolabeled for α-tubulin. We observed different organizations of this cytoskeletal component between clones, which could account for STMN transfectants shape; however, the density of MTs was not modified (Fig. 5, B, D, and F).

Stathmin level affects two-dimensional motility

Being interested in studying stathmin-mediated migration, we performed a first round of experiments to determine whether differences of stathmin expression could modulate motility, here defined as two-dimensional movement, or chemokinesis. The nuclear coordinates of single cells were measured every 30 min for 3 h and the mean speed of cell movement was calculated. Our results show different chemokinetic responses: stathmin overexpression induced a significant increase in motility (23.6 μm/h) when compared with the pIRES (13.5 μm/h), whereas no significant difference between STMN− (12.6 μm/h) and pIRES cells motility was detected.

Stathmin level modifies aggregation ability

Parental GN-11, pIRES, and STMN− cells, in subconfluent culture conditions, exhibit cell-cell adhesion, whereas STMN+ cells grow exclusively as single cells.

Using the hanging drop approach (35), we showed that, unlike pIRES and STMN−, STMN+ cells were scattered and spread into the collagen gel and do not aggregate at all (Fig. 7A). To further investigate a possible role for stathmin in the impairment of cell-cell adhesion, we analyzed N-cadherin protein expression in the different clones. As shown in Fig. 7B, we found that STMN− cells expressed higher levels of full-length N-cadherin (130 kDa) compared with pIRES cells and a truncated (95 kDa) isoform (42), which was absent in the STMN+ and pIRES clones. Concurrently with the above observations, STMN+ cells express very low level of full-length N-cadherin (130 kDa).

Stathmin level modifies three-dimensional basal and chemotactic motility

To evaluate the ability of STMN transfectants to migrate in a three-dimensional environment, we assayed basal motility and chemotaxis using transwell assay, a common approach for sensitive measurement of cellular response to specific chemotropic signals (43, 44). In previous studies, we and others (36, 45) have shown that GN-11 cells display migratory activity. To determine whether stathmin expression was involved in GN-11 basal cell migration, transwell assays were performed with STMN+ and STMN− clones in SFM. The statistical analysis of migrated cells after 6 h of

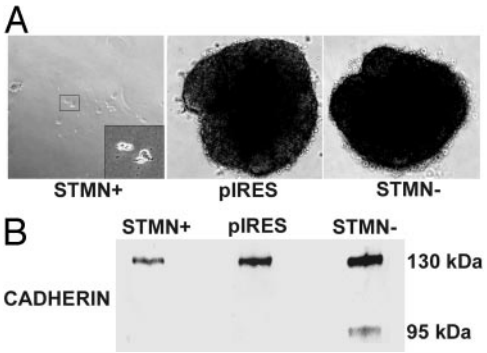

FIG. 7. A, Aggregation assays of STMN+, pIRES, and STMN− cells. pIRES and STMN− cells form aggregates in collagen gel (hanging drop technique), whereas STMN+ cells are scattered and spread into the collagen gel. The inset shows, at higher magnification, STMN+ cells not forming aggregates. B, N-cadherin protein expression in STMN clones. STMN− cells, compared with pIRES, express high level of full-length N-cadherin (130 kDa) and, in addition, the induction of a truncated (95 kDa) isoform. Concurrently, STMN+ cells express very low level of full-length N-cadherin (130 kDa).

incubation clearly showed the different migratory activity of pIRES, STMN+ and STMN− clones (Fig. 8). STMN+ cells exhibited a significant increase in cell migration activity when compared with pIRES, whereas, in the same experimental conditions, STMN− cells showed a significant decrease.

STMN clones were then assayed for their ability to respond to the chemotactic molecule, HGF/SF. We have previously shown that GN-11 cells express the tyrosine kinase receptor c-Met and respond to the chemotactic stimulus induced by its ligand, HGF/SF (45). Cells were seeded in the transwell and exposed to a source of HGF/SF (50 ng/ml; Ref. 45), which was added in the bottom chamber (see *Materials and Methods*). As shown in Fig. 8A, all clones responded significantly to HGF/SF treatment, with an increase in cell migration compared with SFM treatment. Noteworthy, the amplitude of the response is correlated to the basal motility of each clone. In addition, STMN+ cells displayed increased cell motility both in SFM condition and in the presence of HGF/SF when compared with pIRES cells. Concurrently, STMN− cells displayed decreased cell motility both in SFM condition and in the presence of HGF/SF when compared with pIRES cells. Finally, no significant differences in c-Met expression were observed between GN-11, pIRES, STMN− and STMN+ cells, as detected by RT-PCR and immunoblotting analyses (Fig. 8B).

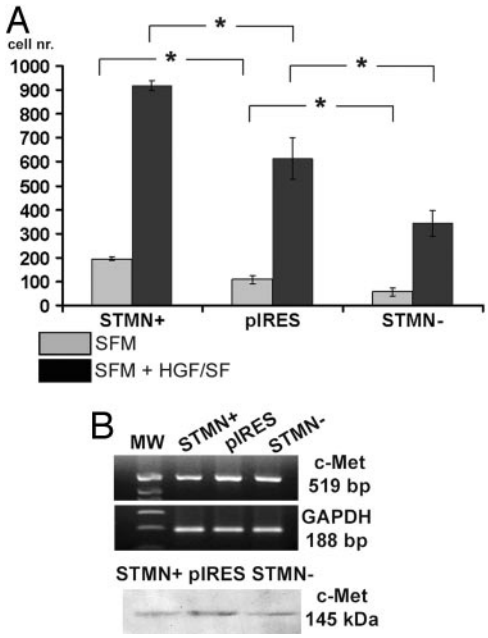

FIG. 8. A, Three-dimensional migration assay. Chemotactic response of STMN+, pIRES and STMN− cells, performed using the transwell method: 10^5 cells were allowed to migrate for 6 h in the absence or in the presence of 50 ng/ml HGF/SF. Each value represents the mean ± SD of three experiments in triplicate. All clones respond significantly to HGF/SF treatment, with an increase in cell migration when compared with untreated conditions and the amplitude of the response is correlated to the basal motility of each clone. STMN+ cells, when compared with pIRES cells, display an increased motility both in SFM condition and in the presence of HGF/SF. STMN− cells, when compared with pIRES cells, display a decreased motility both in SFM condition and in the presence of HGF/SF. B, c-Met expression in STMN transfectants extracts. Total mRNAs were assayed by RT-PCR for c-Met, GAPDH served as control. Predicted amplicons molecular weights were: 519 bp for c-Met and 188 bp for GAPDH. Protein extracts were analyzed for c-Met (145 kDa) expression. MW, Molecular weight.

Discussion

In the present paper, we show that the MT-associated phosphoprotein stathmin is expressed *in vivo* in migrating GnRH producing cells during development as well as *in vitro*, in the GN-11 cells (30). In addition, we demonstrate that the modulation of stathmin expression significantly affects shape and motility of GN-11 cells.

During central nervous system (CNS) development and in the adult, MTs are involved in numerous intracellular events, such as proliferation, differentiation, and migration. In neurons, MTs play specific roles in axonal outgrowth, pathfinding, and synapse formation, as well as in axonal and dendritic transport (46). We have focused our interest on the MT-associated protein stathmin and investigated its role as one of the possible regulators of these events.

Stathmin phosphoprotein interferes with MT assembly and plays an important role in the regulation of MT dynamics during cell cycle progression. It is also highly expressed in early embryos (47–49), gonads (50), and in particular it has been shown to be present in several brain areas (28, 51–54), but its function in the CNS is not completely clear. Stathmin has also been proposed to act as an intracellular relay for extracellular signals (55) and many proteins, apart from tubulin, have been identified as target/partners for stathmin (56–58). A stathmin gene has also been identified in *Drosophila* (59); like the mammalian protein, *Drosophila* stathmin interferes with MT dynamics both *in vitro* and *in vivo*. Furthermore, functional inactivation of the stathmin gene in *Drosophila*, by RNA interference, leads to abnormal germ cell migration in the embryo and to dramatic defects in the formation of the nervous system, supporting a direct role of stathmin in these essential biological processes.

In mammals, stathmin immunostaining in the CNS localizes to immature olfactory neurons as well as to migrating cells generated from the OE, supporting the role of this protein in neurogenesis and cell migration (29). Although stathmin had been associated with numerous cell events, its biological role remained elusive as inactivation of the stathmin gene in mouse resulted in no clear deleterious phenotype (60). In a recent study, microinjections of stathmin antisense oligonucleotides in the lateral ventricle of adult rats, inhibited interneuronal migration from the subventricular zone to the olfactory bulb via rostral migratory stream (61).

We now have evidence, by consecutive and simultaneous double immunohistochemical analyses, that stathmin is expressed by GnRH neurons. This expression is specific of the migration step and ceases as soon as GnRH neurons reach their final hypothalamic destination. Thus, stathmin expression in GnRH neurons is temporally and spatially regulated during mouse development. Based on the preexisting literature and on the present results, we postulated that stathmin is involved in the control of migration properties of GnRH neurons. To determine whether a correlation might exist between stathmin expression level and migratory capabilities of GnRH neurons, we moved to GN-11 cell line. This cell

line was derived from a tumor developed in the cribriform plate of mouse embryos (30). GN-11 cells retain many of the morphological and behavioral features of migrating neurons (45, 59, 62). Therefore, this cell line provides a suitable model to study the involvement of stathmin in the regulation of GnRH neuronal migration.

Complete stathmin cDNA was cloned both in sense and antisense orientation in pIRES vector and stably transfected into GN-11 cells. Selected clones showed overexpression (STMN+) or down-regulation (STMN−) of stathmin compared with control clones. As already demonstrated for K562 erythroleukemia cells (23) and for human embryonic kidney 293 cells (63), the alteration of stathmin expression in GN-11 cells induces modifications in proliferation activity, confirming a role for stathmin as mitotic regulator in this cell line. Interestingly, beside its effect on proliferation, modifications of stathmin expression caused also changes in GN-11 cell morphology. High levels of stathmin expression induced the cells to adopt the typical morphology of *in vivo* GnRH migrating neurons (64), with elongated and spindle-shaped cell bodies and the extension of a leading and a trailing process. Cells expressing low levels of stathmin showed neurite-like outgrowth and displayed a multipolar morphology. The significance of these morphological observations was evaluated and confirmed by quantitative analysis of parameters such as area, perimeter, and shape.

Bidimensional analysis of cell motility revealed a significant increase in the speed of STMN+ cells when compared with control and STMN− cells. Interestingly, STMN+ cells did not establish any contact with each other, suggesting a possible variation of the expression of cell-cell adhesion molecules. Previous studies have shown that cell adhesion molecules, including N-cadherins, are implicated in the formation of the nervous system (65). Their expression is highly regulated during nervous system development to control cell migration, neurite outgrowth, fasciculation, and synaptogenesis. It has also been demonstrated that down-regulation of cadherin's expression hastened the migration of newly generated neurons produced in the subependymal zone (66). In other model systems, inactivation of the cadherin adhesion complex seems to be associated with cell dedifferentiation, invasion, and regional metastasis (67, 68), all processes requiring cell motility. Based on these data, we focused our attention on the adhesive properties of GN-11 cells and analyzed the expression of N-cadherins in our experimental model. Interestingly, we found out that the expression patterns of stathmin and N-cadherins are inversely correlated: overexpression of stathmin induces a down-regulation of N-cadherin expression and the loss of the ability to form cell aggregates by the hanging-drop technique, whereas down-regulation of stathmin is accompanied by an increase in N-cadherin protein expression and cell-cell adhesion. A correlation between stathmin and cadherins has been previously highlighted by Balogh and co-workers (69), who showed that cell-cell contacts, probably mediated by cadherins, may be important in the control of stathmin expression.

Using transwell assay, we showed that spontaneous migratory activity of GN-11 cells is sensitive to stathmin content. Indeed, transfection of GN-11 cells with stathmin sense construct significantly increases basal migration, whereas down-regulation of stathmin expression by antisense construct transfection inhibits such activity when compared with control cells. These results are in accordance with those of Jin and co-workers (61) demonstrating a role for stathmin in the rostral migratory stream neuronal migration by ventricular antisense oligonucleotide injection.

HGF/SF motogenic activity has been demonstrated in several cell lines, during embryogenesis, and in metastatic tissues (for a review see Ref. 38). In the developing CNS, HGF/SF and its receptor c-Met are involved in the migration of cortical (70) and GnRH neurons (45). In addition, GN-11 cells have been previously shown to express c-Met and display chemotactic responsiveness to HGF/SF stimulation (45). Because the level of c-Met expression is not affected by stathmin content, the migratory activity of STMN+, pIRES, and STMN− transfectants has been measured under the exposure to HGF/SF. A chemotactic response to HGF/SF is observed for all transfectants and the amplitude of the response correlates to stathmin content. The activation of c-Met receptor by HGF/SF leads to the recruitment, among others, of the scaffolding protein Grb2, which activates Rac-1 (38). On the other hand, the activation of Rac-1-dependent kinase has been recently demonstrated to regulate stathmin activity at the leading edge of migrating cells (71, 72). Therefore, a challenging hypothesis that will deserve further investigation is the regulation of stathmin activity by Rac-1-dependent kinase in GN-11 cells in response to HGF/SF.

The temporal expression of stathmin protein by migrating GnRH neurons is in accordance with the *in vitro* findings that we obtained using GN-11 cell line. In addition, once GnRH neurons have reached their final hypothalamic destinations, they no longer express stathmin and complete their differentiation to become integral components of the hypothalamic-pituitary-gonadal axis, which is essential for establishment of reproductive competence. Whether down-regulation of stathmin expression is a necessary step for GnRH neuronal differentiation or, inversely, a consequence of the differentiation program of the neuroendocrine cells, deserves further investigations.

Acknowledgments

Received July 27, 2004. Accepted December 13, 2004.

Address all correspondence and requests for reprints to: Isabelle Perroteau, Department of Human and Animal Biology, University of Torino, Via Accademia Albertina 13, 10123 Torino, Italy. E-mail: isabelle.perroteau@unito.it.

This work was supported by Compagnia di San Paolo and FIRB PRONEURO (FIRB RBNE01WY7P).

References

1. **Sagrillo CA, Grattan DR, McCarthy M, Selmanoff M** 1996 Hormonal and neurotransmitter regulation of GnRH gene expression and related reproductive behaviours. Behav Genet 26:241–277
2. **Silverman A-J, Livne I, Witchin JV** 1994 The gonadotropin releasing hormone GnRH neuronal system: immunocytochemistry and in situ hybridization. In: Knobill E, Neil JD, eds. Physiology of reproduction. New York: Raven Press; 1683–1710
3. **Wray S** 2002 Development of gonadotropin-releasing hormone-1 neurons. Front Neuroendocrinol 23:292–316
4. **Schwanzel-Fukuda M, Pfaff DW** 1989 Origin of luteinizing hormone-releasing hormone neurons. Nature 338:161–164
5. **Wray S, Grant P, Gainer H** 1989 Evidence that cells expressing luteinizing

hormone-releasing hormone mRNA in the mouse are derived from progenitor cells in the olfactory placode. Proc Natl Acad Sci USA 86:8132–8136
6. **Wray S, Key S, Qualls R, Fueshko SM** 1994 A subset of peripherin positive olfactory axons delineates the luteinizing hormone releasing hormone neuronal migratory pathway in developing mouse. Dev Biol 166:349–354
7. **Yoshida K, Rutishauser U, Crandall JE, Schwarting GA** 1999 Polysialic acid facilitates migration of luteinizing hormone-releasing hormone neurons on vomeronasal axons. J Neurosci 19:794–801
8. **Ronnekleiv OK, Resko JA** 1990 Ontogeny of gonadotropinreleasing hormone-containing neurons in early foetal development of rhesus macaques. Endocrinology 126:498–511
9. **Quanbeck C, Sherwood NM, Millar RP, Terasawa E** 1997 Two populations of luteinizing hormone-releasing neurons in the forebrain of the rhesus macaque during embryonic development. J Comp Neurol 380:293–309
10. **Schwanzel-Fukuda M, Crossin KL, Pfaff DW, Bouloux PM, Hardelin JP, Petit C** 1996 Migration of luteinizing hormone releasing hormone (LHRH) neurons in early human embryos. J Comp Neurol 366:547–557
11. **Wehrle-Haller B, Imhof BA** 2003 Actin, microtubules and focal adhesion dynamics during cell migration. Int J Biochem Cell Biol 35:39–50
12. **Rakic P, Knyihar-Csillik E, Csillik B** 1996 Polarity of microtubule assemblies during neuronal cell migration. Proc Natl Acad Sci USA 93:9218–9222
13. **Sobel A** 1991 Stathmin: a relay phosphoprotein for multiple signal transduction? Trends Biochem Sci 16:301–305
14. **Gavet O, Ozon S, Manceau V, Lawler S, Curmi P, Sobel A** 1998 The stathmin phosphoprotein family: intracellular localization and effects on the microtubule network. J Cell Sci 111(Pt 22):3333–3346
15. **Holmfeldt P, Larsson N, Segerman B, Howell B, Morabito J, Cassimeris L, Gullberg M** 2001 The catastrophe-promoting activity of ectopic Op18/stathmin is required for disruption of mitotic spindles but not interphase microtubules Mol Biol Cell 12:73–83
16. **Kuntziger T, Gavet O, Manceau V, Sobel A, Bornens M** 2001 Stathmin/Op18 phosphorylation is regulated by microtubule assembly. Mol Biol Cell 12: 437–448
17. **Iancu C, Mistry SJ, Arkin S, Wallenstein S, Atweh GF** 2001 Effects of stathmin inhibition on the mitotic spindle. J Cell Sci 114:909–916
18. **Mistry SJ, Atweh GF** 2001 Stathmin inhibition enhances okadaic acid-induced mitotic arrest: a potential role for stathmin in mitotic exit. J Biol Chem 276: 31209–31215
19. **Mistry SJ, Atweh GF** 2002 Role of stathmin in the regulation of the mitotic spindle: potential applications in cancer therapy. Mt Sinai J Med 69:299–304
20. **Cassimeris L** 2002 The oncoprotein 18/stathmin family of microtubule destabilizers. Curr Opin Cell Biol 14:18–24
21. **Melander Gradin H, Marklund U, Larsson N, Chatila TA, Gullberg M** 1997 Regulation of microtubule dynamics by Ca21/calmodulin-dependent kinase IV/Gr-dependent phosphorylation of oncoprotein 18. Mol Cell Biol 17:3459–3467
22. **Brattsand G, Marklund U, Nylander K, Roos G, Gullberg M** 1994 Cell-cycle-regulated phosphorylation of oncoprotein 18 on Ser16, Ser25 and Ser38. Eur J Biochem 22:359–368
23. **Luo XN, Mookerjee B, Ferrari A, Mistry S, Atweh GF** 1994 Regulation of phosphoprotein p18 in leukemic cells. Cell cycle regulated phosphorylation by p34cdc2 kinase. J Biol Chem 269:10312–10318
24. **Marklund U, Brattsand G, Shingler V, Gullberg M** 1993 Serine 25 of oncoprotein 18 is a major cytosolic target for the mitogen-activated protein kinase. J Biol Chem 268:15039–15047
25. **Marklund U, Larsson N, Brattsand N, Osterman O, Chatila TA, Gullberg M** 1994 Serine 16 of oncoprotein 18 is a major cytosolic target for the Ca21/calmodulin-dependent kinase-Gr. Eur J Biochem 225:53–60
26. **Altman J, Das GD** 1965 Post-natal origin of microneurones in the rat brain. Nature 207:953–956
27. **Brunjes PC, Frazier LL** 1986 Maturation and plasticity in the olfactory system of vertebrates. Brain Res 396:1–45
28. **Camoletto P, Peretto P, Bonfanti L, Manceau V, Sobel A, Fasolo A** 1997 The cytosolic phosphoprotein stathmin is expressed in the olfactory system of the adult rat. Neuroreport 8:2825–2829
29. **Camoletto P, Colesanti A, Ozon S, Sobel A, Fasolo A** 2001 Expression of stathmin and SCG10 proteins in the olfactory neurogenesis during development and after lesion in the adulthood. Brain Res Bull 54:19–28
30. **Radovick S, Wray S, Lee E, Nicols DK, Nakayama Y, Weintraub BD, Westphal H, Cutler Jr GB, Wondisford FE** 1991 Migratory arrest of gonadotropin-releasing hormone neurons in transgenic mice. Proc Natl Acad Sci USA 88: 3402–3406
31. **Sambrook J, Fritsch EF, Maniatis T** 1999 Molecular cloning: a laboratory manual. 2nd ed. Cold Spring Harbor, NY: Cold Spring Harbor Laboratory Press
32. **Chan AM, King HWS, Deakin EA, Tempest PR, Hilkens J, Kroezen V, Edwards DR, Wills AJ, Brooks P, Cooper CS** 1988 Characterization of the mouse met proto-oncogene. Oncogene 2:593–599
33. **Gillies RJ, Didier N, Denton M** 1986 Determination of cell number in monolayer cultures. Anal Biochem 159:109–113
34. **Kueng W, Silber E, Eppenberger U** 1989 Quantification of cells cultured on 96-well plates. Anal Biochem182:16–19
35. **Kennedy TE, Serafini T, de la Torre JR, Tessier-Lavigne M** 1994 Netrins are diffusible chemotropic factors for commissural axons in the embryonic spinal cord. Cell 78:425–435
36. **Maggi R, Pimpinelli F, Molteni L, Milani M, Martini L, Piva F** 2000 Immortalized luteinizing hormone-releasing hormone neurons show a different migratory activity *in vitro.* Endocrinology 141:2105–2112
37. **Giordano S, Maffe A, Williams TA, Artigiani S, Gual P, Bardelli A, Basilico C, Michieli P, Comoglio PM** 2000 Different point mutations in the met oncogene elicit distinct biological properties. FASEB J 14:399–406
38. **Birchmeier C, Birchmeier W, Gherardi E, Vande Woude GF** 2003 Met, metastasis, motility and more. Nat Rev Mol Cell Biol 4: 915–925
39. **Olayioye MA, Neve RM, Lane HA, Hynes NE** 2000 The ErbB signalling network: receptor heterodimerization in development and cancer. EMBO J 19:3159–3167
40. **Yarden Y, Sliwkowski MX** 2001 Untangling the ErbB signalling network. Nat Rev Mol Cell Biol 2:127–137
41. **Hilger-Eversheim K, Moser M, Schorle H, Buettner R** 2000 Regulatory roles of AP-2 transcription factors in vertebrate development, apoptosis and cell-cycle control. Gene 260:1–12
42. **Kido M, Obata S, Tanihara H, Rochelle JM, Seldin MF, Taketani S, Suzuki ST** 1998 Molecular properties and chromosomal location of cadherin-8. Genomics 48:186–194
43. **Isenberg JS** 2003 Inhibition of nitric oxide synthase (NOS) conversion of L-arginine to nitric oxide (NO) decreases low density mononuclear cell (LD MNC) trans-endothelial migration and cytokine output. J Surg Res 114:100–106
44. **Prest SJ, Rees RC, Murdoch C, Marshall JF, Cooper PA, Bibby M, Li G, Ali SA** 1999 Chemokines induce the cellular migration of MCF-7 human breast carcinoma cells: subpopulations of tumour cells display positive and negative chemotaxis and differential in vivo growth potentials. Clin Exp Metastasis 17:389–396
45. **Giacobini P, Giampietro C, Fioretto M, Maggi R, Cariboni A, Perroteau I, Fasolo A** 2002 Hepatocyte growth factor/scatter factor facilitates migration of GN-11 immortalized LHRH neurons. Endocrinology 143:3306–3315
46. **Dent EW, Gertler FB** 2003 Cytoskeletal dynamics and transport in growth cone motility and axon guidance. Neuron 40:209–227
47. **Doye V, Le Gouvello S, Dobransky T, Chneiweiss H, Beretta L, Sobel A** 1992 Expression of transfected stathmin cDNA reveals novel phosphorylated forms associated with developmental and functional cell regulation. Biochem J 287(Pt 2):549–554
48. **Koppel J, Rehak P, Baran V, Vesela J, Hlinka D, Manceau V, Sobel A** 1999 Cellular and subcellular localization of stathmin during oocyte and preimplantation embryo development. Mol Reprod Dev 53:306–317
49. **Soodeen-Karamath S, Gibbins AM** 2000 The chicken stathmin gene and its expression in the embryo. Biochem Cell Biol 78:703–713
50. **Guillaume E, Evrard B, Com E, Moertz E, Jegou B, Pineau C** 2001 Proteome analysis of rat spermatogonia: reinvestigation of stathmin spatio-temporal expression within the testis. Mol Reprod Dev 60:439–445
51. **Amat JA, Fields Kay L, Schubart Ulrich K** 1991 Distribution of phosphoprotein p19 in rat brain during ontogeny: stage-specific expression in neurons and glia. Dev Brain Res 60:205–218
52. **Peschanski M, Hirsch E, Dusart I, Doye V, Marty S, Manceau V, Sobel A** 1993 Stathmin: cellular localization of a major phosphoprotein in the adult rat and human CNS. J Comp Neurol 337:655–668
53. **Pellier-Monnin V, Astic L, Bichet S, Riederer BM, Grenningloh G** 2001 Expression of SCG10 and stathmin proteins in the rat olfactory system during development and axonal regeneration. J Comp Neurol 433:239–254
54. **Gavet O, El Massari S, Ozon S, Sobel A** 2002 Regulation and subcellular localization of the microtubule-destabilizing stathmin family phosphoproteins in cortical neurons. J Neurosci Res 68:535–550
55. **Sobel A, Boutterin MC, Beretta L, Chneiweiss H, Doye V, Peyro-Saint-Paul H** 1989 Intracellular substrates for extracellular signaling. Characterization of a ubiquitous, neuron-enriched phosphoprotein (stathmin). J Biol Chem 264:3765–3772
56. **Li L, Cohen SN** 1996 Tsg101: a novel tumor susceptibility gene isolated by controlled homozygous functional knockout of allelic loci in mammalian cells. Cell 85:319–329
57. **Maucuer A, Camonis JH, Sobel A** 1995 Stathmin interaction with a putative kinase and coiled-coil-forming protein domains. Proc Natl Acad Sci USA 92:3100–3104
58. **Maucuer A, Ozon S, Manceau V, Gavet O, Lawler S, Curmi P, Sobel A** 1997 KIS is a protein kinase with an RNA recognition motif. J Biol Chem 1997 272:23151–23156
59. **Ozon S, Guichet A, Gavet O, Roth S, Sobel A** 2002 Drosophila stathmin: a microtubule-destabilizing factor involved in nervous system formation. Mol Biol Cell 13:698–710
60. **Liedtke W, Leman EE, Fyffe RE, Raine CS, Schubart UK** 2002 Stathmin-deficient mice develop an age-dependent axonopathy of the central and peripheral nervous systems. Am J Pathol 160:469–480
61. **Jin K, Mao XO, Cottrell B, Schilling B, Xie L, Row RH, Sun Y, Peel A, Childs J, Gendeh G, Gibson BW, Greenberg DA** 2004 Proteomic and immunochemical characterization of a role for stathmin in adult neurogenesis. FASEB J 18:287–299

62. **Pimpinelli F, Redaelli E, Restano-Cassulini R, Curia G, Giacobini P, Cariboni A, Wanke E, Bondiolotti GP, Piva F, Maggi R** 2003 Depolarization differentially affects the secretory and migratory properties of two cell lines of immortalized luteinizing hormone-releasing hormone (LHRH) neurons. Eur J Neurosci 18:1410–1418
63. **Lawler S, Gavet O, Rich T, Sobel A** 1998 Stathmin overexpression in 293 cells affects signal transduction and cell growth. FEBS Lett 421:55–60
64. **Way S, Nieburgs A, Elkabes S** 1989 Spatiotemporal cell expression of luteinizing hormone-releasin hormone in the prenatal mouse: evidence for an embryonic origin in the olfactory placode. Brain Res Dev Brain Res 46:309–318
65. **Akitaya T, Bronner-Fraser M** 1992 Expression of cell adhesion molecules during initiation and cessation of neural crest cell migration. Dev Dyn 194: 12–20
66. **Barami K, Kirschenbaum B, Lemmon V, Goldman SA** 1994 N-cadherin and Ng-CAM/8D9 are involved serially in the migration of newly generated neurons into the adult songbird brain. Neuron 13:567–582
67. **Moersig W, Horn S, Hilker M, Mayer E, Oelert H** 2002 Transfection of E-cadherin cDNA in human lung tumor cells reduces invasive potential of tumors. Thorac Cardiovasc Surg 50:45–48
68. **Bremnes RM, Veve R, Hirsch FR, Franklin WA** 2002 The E-cadherin cell-cell adhesion complex and lung cancer invasion, metastasis, and prognosis. Lung Cancer 36:115–124
69. **Balogh A, Mege RM, Sobel A** 1996 Growth and cell density-dependent expression of stathmin in C2 myoblasts in culture. Exp Cell Res 224: 8–15
70. **Powell EM, Mars WM, Levitt P** 2001 Hepatocyte growth factor/scatter factor is a motogen for interneurons migrating from the ventral to dorsal telencephalon. Neuron 30:79–89
71. **Niethammer P, Bastiaens P, Karsenti E** 2004 Stathmin-tubulin interaction gradients in motile and mitotic cells. Science 303:1862–1866
72. **Wittmann T, Bokoch GM, Waterman-Storer CM** 2004 Regulation of microtubule destabilizing activity of Op18/stathmin downstream of Rac1. J Biol Chem 279:6196–6203

***Endocrinology* is published monthly by The Endocrine Society (http://www.endo-society.org), the foremost professional society serving the endocrine community.**